Reversal modes in arrays of interacting magnetic Ni nanowires: Monte Carlo simulations and scaling technique

M. Bahiana and F. S. Amaral
Instituto de Física, Universidade Federal do Rio de Janeiro Caixa Postal 68528, Rio de Janeiro, RJ, Brazil, 21945-970

S. Allende and D. Altbir
Departamento de Física, Universidad de Santiago, Casilla 307, Santiago 2, Chile
(Received 23 June 2006; revised manuscript received 27 September 2006; published 9 November 2006)

The effect of dipolar interactions in hexagonal arrays of Ni nanowires has been investigated by means of Monte Carlo simulations combined with a scaling technique, which allows the investigation of the internal structure of the wires. A strong dependence of the coercivity and remanence on the distance between wires has been observed. At intermediate packing densities the coercivity exhibits a maximum, higher than the noninteracting value. This behavior, experimentally observed, has been explained on grounds of the interwire dipolar interactions. Also, different reversal modes of the magnetization have been identified.

DOI: 10.1103/PhysRevB.74.174412 PACS number(s): 75.75.+a, 75.60.Ej, 75.60.Jk

I. INTRODUCTION

In recent years, a great deal of attention has been focused on the study of regular arrays of magnetic particles with dimensions in the nanometer range. These particles have potential applications in nonvolatile magnetic memory devices or high-resolution magnetic field sensors[1] and arrays of discrete patterned magnetic elements, such as magnetic wires, rings, and dots, have been proposed as a new generation of ultrahigh density patterned magnetic storage media.[2] Experimental and theoretical results over the past years show that there are many factors, such as geometry, anisotropy, and magnetic interactions among the particles, that influence the magnetic behavior of the systems. The question of how the interelement spacing affects the magnetic properties of an array is relevant in understanding and interpreting experimental results since this spacing can influence both the magnetization reversal mechanism and the internal magnetic domain structures. The effect of interparticle interactions is in general complicated by the fact that the dipolar fields depend upon the magnetization state of each element, which in turn depend upon the fields due to adjacent elements. Therefore modeling of such systems is often subject to strong simplifications like, for example, considering monodomain particles. In the specific case of wires, Sampaio *et al.*[3] have described an array of microwires as a one-dimensional array of Ising-type magnetic moments subject to an anisotropy field, representing the wire shape anisotropy, and with the dipolar interaction taken into account as a field depending on the orientation of the participating magnetic moments. Hysteresis curves with some of the features observed in experiments were obtained by Monte Carlo simulations. A more realistic model was presented in Ref. 4 to describe one- and two-dimensional arrays of microwires. In this case the magnetic moments were allowed to point at any direction on the plane, and dipolar interactions have been directly calculated. This approach provides a description limited to very long wires in a weakly interacting regime, excluding the exploration of many interesting issues. Models for wires with nonuniform magnetization have been restricted to micromagnetic calculations.[5–7] The introduction of internal degrees of freedom enables mapping the field in the vicinity of the wire[7] and identifying a corkscrew reversal mode.[5]

In this paper we develop Monte Carlo simulations for an array of nanowires in which the internal structure of each wire is taken into account. We focus on arrays of nanowires created by electrodeposition of nickel in porous alumina membranes.[8] This fabrication technique produces hexagonal arrays of nanowires with long-range ordering, and well controlled center to center distance (D), diameter (d), and length (ℓ). Typical values are $d=10-100$ nm, $\ell=0.1-1$ μm and $D=30-100$ nm. More frequently studied are wires with aspect ratios $\ell/d>10$ in order to enforce the bit character of individual elements, so we also consider nanowires with this characteristic. Experimentally it is possible to observe that the coercive field strongly depends on the ratio d/D, indicating that the reversal process is greatly affected by magnetostatic interaction among wires.[9] This effect is observed in several experiments, in which the hysteresis curves for membranes with different packing densities are measured.[8–10] Wires in the above-mentioned range of sizes have at least 10^8 atoms, and since dipolar interactions must be considered in those systems, numerical simulations at the atomic level are out of reach with the present computational facilities. In order to circumvent this difficulty, we make use of a scaling technique presented by d'Albuquerque *et al.*,[11] which was applied to the calculation of the phase diagram of cylindrical particles. In this approach the number of particles is reduced to a value suitable for numerical calculations, which decreases the dipolar field felt by each particle. The exchange coupling constant is then scaled down in order to keep the correct balance between magnetostatic and exchange energies, responsible for domain formation and reversal mechanisms. This technique, combined with standard Monte Carlo simulations, has been used in the study of nanometric elements, providing results otherwise unattainable with this approach.[12,13]

Modeling an array with macroscopic dimensions, even with the scaling procedure, is not possible due to the large number of wires. In order to extract information about the

reversal process taking into account the interaction with neighboring wires and, at the same time, use reasonable computational time, we have studied a hexagonal cell with seven wires, considering the central wire, which interacts with the full number of first neighboring wires, as representative of a typical element of a macroscopic array. Monte Carlo simulations were used to calculate the hysteresis curve for cells with different interwire spacing. The behavior of the coercivity and the reversal modes for weak and strong interacting limits were analyzed.

II. MODEL

The internal energy E_{tot} of a wire array with N magnetic moments can be written as

$$E_{tot} = \sum_{i=1}^{N} \sum_{j>i}^{N} (E_{ij} - J\hat{\mu}_i \cdot \hat{\mu}_j) + E_K + E_H, \tag{1}$$

where E_{ij} is the dipolar energy given by

$$E_{ij} = \frac{\vec{\mu}_i \cdot \vec{\mu}_j - 3(\vec{\mu}_i \cdot \hat{n}_{ij})(\vec{\mu}_j \cdot \hat{n}_{ij})}{r_{ij}^3}. \tag{2}$$

r_{ij} is the distance between the magnetic moments $\vec{\mu}_i$ and $\vec{\mu}_j$, and $\hat{n}_{ij}$ the unit vector along the direction that connects the two magnetic moments. J is the exchange coupling constant between nearest neighbors, and $\hat{\mu}_i$ is the unit vector along the direction of $\vec{\mu}_i$. E_K is a cubic crystalline anisotropy term which can be written as $E_K = K\Sigma_{i=1}^{N}[\alpha_i^2\beta_i^2 + \beta_i^2\gamma_i^2 + \gamma_i^2\alpha_i^2]$, where $(\alpha_i, \beta_i, \gamma_i)$ are the direction cosines of $\vec{\mu}_i$ referred to the cube axis,[14] and $E_H = -\Sigma_{i=1}^{N}\vec{\mu}_i \cdot \vec{H}$ is the contribution of the external field.

In order to compare our simulations with experimental results on granular Ni systems, we have considered $|\vec{\mu}_i| = \mu = 0.615\mu_B$, the lattice parameter $a_0 = 3.52$ Å, $K = 2 \times 10^5$ erg/cm^3, and $J = 1600$ kOe/μ_B.[14] The wires have diameter $d = 30$ nm, length $\ell = 1$ μm, and were built along the [110] direction of a fcc lattice comprising about 6×10^9 atoms. In order to reduce the number of interacting atoms, we make use of the scaling technique presented before,[11] applied to the calculation of the phase diagram of cylindrical particles of height ℓ and diameter d. The authors showed that such diagram is equivalent to the one for a smaller particle with $d' = d\chi^\eta$ and $\ell' = \ell\chi^\eta$, being $\chi < 1$ and $\eta \approx 0.56$, if the exchange constant is also scaled as $J' = \chi J$. It has also been showed[12] that the scaling relations can be used together with Monte Carlo simulations to obtain a general magnetic state of a nanoparticle. We use this idea starting from the desired value for the total number of interacting particles we can deal with. Based on the computational facilities currently available, we have estimated a total of $N \approx 3500$ to be a reasonable value. With this in mind we have obtained the value $\chi = 8 \times 10^{-4}$, that leads to wires with 504 atoms each.

In what follows we simulate hysteresis curves at temperature $T = 300$ K, using the scaling technique described above. It is important to observe that when measuring a hysteresis loop, the value of the coercivity is affected by the rate at which the external field is varied. Similarly, in simulations of that curve the number of Monte Carlo steps for each value of the field is a critical issue to be defined. We have followed the procedure used by many authors, in which the number of Monte Carlo steps for a particular case is varied until fair agreement with experimental results is obtained.[15–17] Then, the number of Monte Carlo steps is kept fixed and all other variables can be changed. Monte Carlo simulations were carried out using the Metropolis algorithm with local dynamics and single-spin-flip methods.[18] The new orientation of the magnetic moment was chosen arbitrarily with a probability $p = \min[1, \exp(-\Delta E/k_B T)]$, where ΔE is the change in energy due to the reorientation of the magnetic moment, and k_B is the Boltzmann constant. One interesting point to be considered is the effect of scaling on temperature at which the simulations are carried out. Since our goal is to obtain hysteresis curves, we need to figure out how the scaling is affecting the transition between metastable states. The energy landscape of the system is rather complicated due to the dipolar interaction, but in the vicinity of each local minimum we can analyze the transitions as regulated by energy barriers of the form $K_e V$ where K_e is an effective anisotropy constant which takes into account several energy contributions, and V is the volume of the particle. Thermal activated transitions naturally lead to the definition of a blocking temperature $T_B \propto K_e V$,[19] so we use this to relate temperature and size. In order to keep thermal activation process invariant under the scaling transformation, the energy barriers must also be invariant therefore temperature should scale as the volume, that is, $T' = \chi^3 \eta T$. From now on, all results refer to the scaled system.

The hysteresis loops were simulated with the external field in the direction of the wire axis. The initial state had the field $H = 2.0$ kOe, higher than the saturation field, and a configuration in which all the magnetic moments were aligned with the external field. The field was then linearly decreased at a rate of 300 Monte Carlo steps for $\Delta H = 0.01$ kOe. In this way, to go from saturation to the coercive field about 120 000 MC steps are needed. The values of coercivity correspond to an average over, at least, ten independent realizations.

III. RESULTS AND DISCUSSION

Our main concern in this work is to investigate the role of dipolar interactions in wire arrays, specially its effect in the coercivity. Figure 1 shows the hysteresis loops for an isolated nanowire and for the central wire of a cell with spacing $D = 40$ nm. Comparing the curves we can immediately conclude that interaction affects the reversal processes not only in respect to the coercivity values, but also to the shape of the curve. The loop for the isolated wire has a 100% squareness, while the one for the interacting central wire, only 45%. Although not shown in the figure, the curve for the central wire of the $D = 100$-nm array almost coincides with the one for an isolated wire. Similar results have been found by other authors. For example, regular arrays of monodisperse columns have been modeled by Samwell *et al.*[20] and Yshii and Sato.[21] Both papers report analytical calculations of an internal field parameter for nanowires in a membrane.

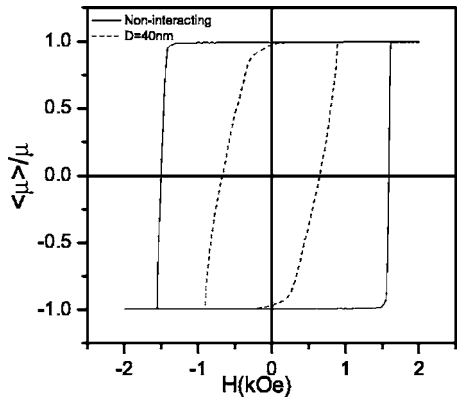

FIG. 1. Hysteresis curves for an isolated wire, and for the central wire of a hexagonal array of 7, with interwire distance $D=40$ nm.

Considering magnetostatic interactions as the only cause of shear in the hysteresis loop, the authors find good agreement with experimental values. Results reported by Sorop *et al.*[22] for Fe nanowires embedded in nanoporous alumina templates reinforce this idea. By examining the wire morphology, and varying the temperature, the authors have discarded the influence of these factors in the shape of the hysteresis loop. The squareness of the hysteresis loop has also been examined by Hwang *et al.*,[23] who fitted experimental curves for arrays of cylindrical Ni particles with a deterministic model in which the cylinders are represented by a single magnetic moment. The arrays have one adjustable parameter, the standard deviation σ for the switching field distribution. By comparing simulations of hysteresis curves for systems of interacting particles and $\sigma=0$, and noninteracting particles and $\sigma\neq 0$, with experimental curves, they were able to conclude that the shear observed is due to interaction among particles.

The effect of interwire spacing on the coercivity can be examined in Fig. 2, where its value is plotted as a function of d/D, for values of D corresponding to almost noninteracting

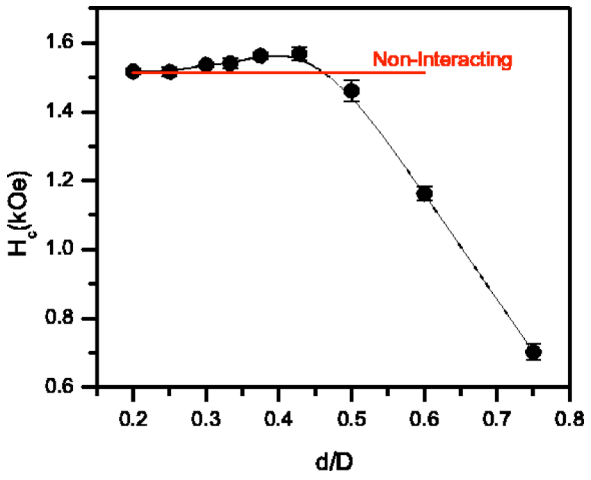

FIG. 2. (Color online) Coercivity of the central wires of a hexagonal array of 7, as a function of the interwire distance D. The wires have diameter $d=30$ nm and length $\ell=10^3$ nm. The solid line is a guide to the eye.

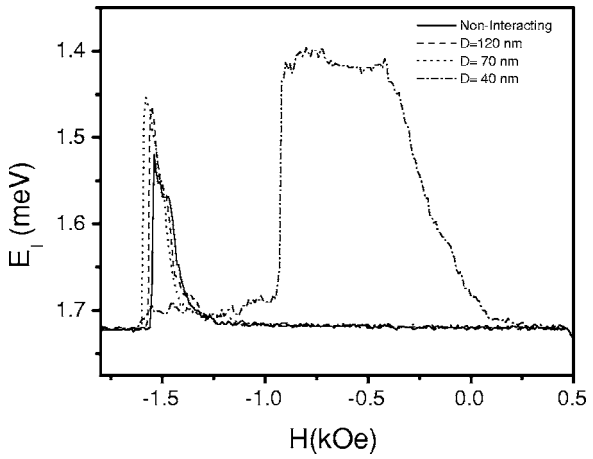

FIG. 3. Internal dipolar energy for the central wire in arrays with $D=40$, 70, and 120 nm, and for an isolated wire, along the hysteresis cycle.

wires, $D=150$ nm, up to strongly interacting ones, for $D=40$ nm. The same behavior was observed in a square arrangement, but with a less pronounced maximum. For comparison, the value obtained for an isolated wire is represented by the horizontal line. The large-D regime coincides with the noninteracting limit, but it is interesting to note that the transition to the strongly interacting regime involves a maximum in coercivity. Since we are looking at the central wire, the curve in Fig. 2 reflects the reversal order of the group of wires. In the limit of noninteracting wires, $D\geqslant 150$ nm ($d/D\leqslant 0.20$) all of them reverse basically at the same time, for $100\ \text{nm}\geqslant D\geqslant 70\ \text{nm}$ ($0.30\leqslant d/D\leqslant 0.43$) the central wire is the last one to revert, and for $60\ \text{nm}\geqslant D\geqslant 40\ \text{nm}$ ($0.50\leqslant d/D\leqslant 0.75$) it is the first one in the reversal process. This increase in stability has also been reported by Hertel.[5] The author has performed micromagnetic simulations of hexagonal arrays of nanowires with fixed geometric parameters. Using our notation, his system is composed by wires with $\ell=1$ μm, $d=40$ nm, and $D=100$ nm, leading to $d/D=0.4$, well within the maximum coercivity region. Hertel examines the effect of increasing the number of wires in the array, as a form of increasing the interaction among wires, and observes that the the reversal of some them occurs because the stray field of neighboring wires adds to the external field and leads to a higher field to which the magnetic moments are effectively exposed as compared to a single nanowire. On the other hand, those wires remaining with magnetization antiparallel to the field are confronted with the stray field of the reversed wires which is oriented opposite to the external field thus reducing the local field. His conclusion is that, in this case, saturation is reached at higher field strength compared to a single wire. The reversal process is regulated, in first order, by the internal dipolar energy of the wire, E_I. This energy corresponds to the dipolar interaction between the magnetic moments within each wire. Figure 3 shows the behavior of E_I along the hysteresis curve, for the central wire of arrays with $D=40$, 70, and 120 nm, and for an isolated wire. For $D>70$ nm the reversal is fast, resulting in a sharp peak in the energy curve, localized at the coercive field. For $D=40$ nm, the reversal starts at zero field, and has a duration about fives times larger.

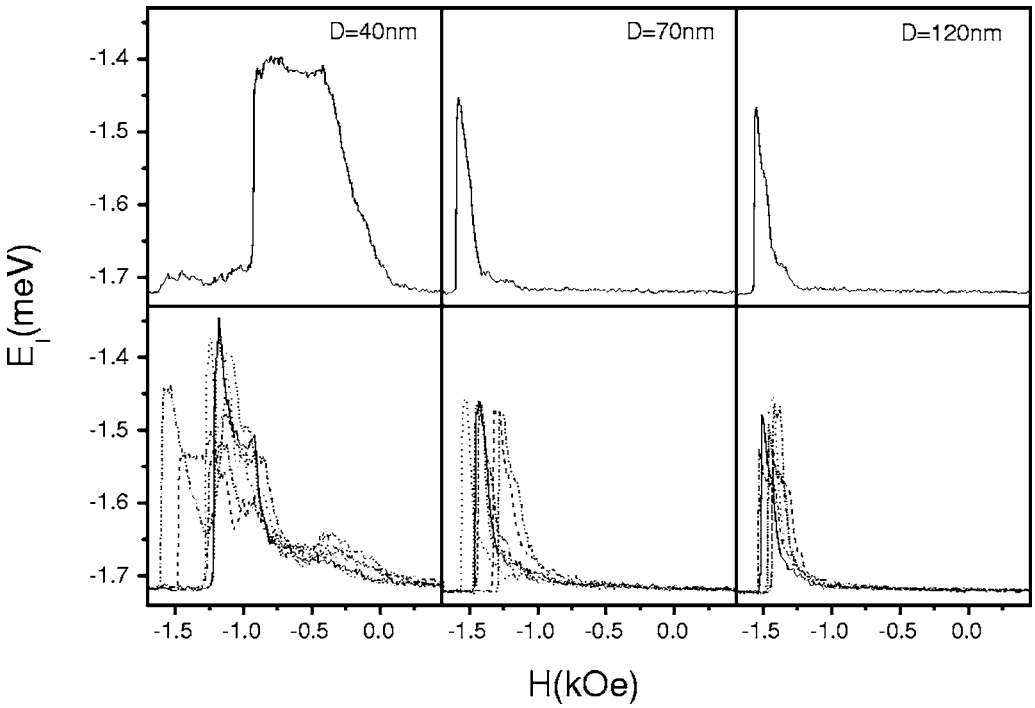

FIG. 4. Internal dipolar energy E_A for individual wires along the hysteresis cycle. The upper line corresponds to the central wire, while the lower one shows the reversal curves for each of the six external wires.

The complexity of the reversal process in strongly interacting arrays is evident when one compares the value of E_I for each wire, for different values of D, along the hysteresis cycle. The upper curves in Fig. 4 illustrate E_I of the central wire for $D=40$, 70, and 120 nm, while the lower curves depict E_I of the six external wires of the array, for the same values of D. For $D=120$ nm, the process consists of a sequence of sharp reversals within an interval of 0.3 kOe. For $D=70$ nm we observe that a variation of about 0.5 kOe is needed to reverse all wires, but it is still possible to identify the reversal of each individual wire. The situation for the strongly interacting array, with $D=40$ nm, is quite different. Each reversal curve has a complicated structure and the superposition is large. Also, the peaks are wider and span a large interval of field values. The reversal of the whole array involves a variation of about 1.6 kOe, and only the reversion of the central wire can be well separated from the others, acting as a trigger to the reversion of the surrounding wires.

Examining the internal structure of each wire, we notice another effect from the interaction. Reversion in isolated wires occurs via nucleation of domain walls at the wire tips, that propagate and merge near the center as found also in micromagnetic simulations.[5] In the $D=40$ nm array we have also observed the nucleation of domain walls at the center of the wire, propagating towards the tips and merging with the walls coming from there. Figure 5 shows two moments of the reversal process for such array. In Fig. 5(a) the central wire has already started to revert and has two domain walls traveling towards the center. A snapshot taken later [Fig. 5(b)] shows three wires completely reverted, and two of the outer wires with nucleation of domain walls in the central part also.

In order to better understand the appearance of the maximum at $D=70$ nm, the relative stability of possible wire configurations must be investigated. For this purpose we have calculated magnetization and energy of the hexagonal array in the absence of external field, assuming that the wires were saturated with magnetization along the wire axis. For $D=40$ nm, the dipolar energy of the central wire is -1.55 meV, while the energy of each outer wire is -1.60 meV. Since the central wire has a higher energy, its reversion is more likely to occur. For $D=70$ nm the energies become -1.66 meV for the central wire and -1.67 meV for the outer ones. In this case the energy difference is not large enough to make the central wire considerably less stable. Actually, as some magnetic moments in the outer wires acquire components transverse to the wire axis, the central wire has its energy low-

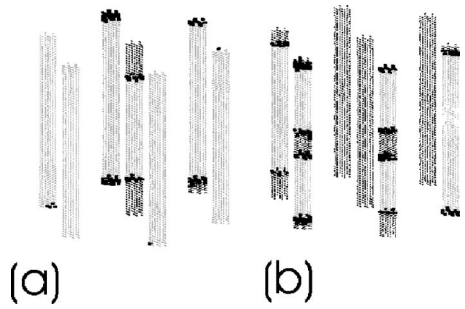

FIG. 5. Reversal process in an array with $D=40$ nm along the hysteresis curve, for two different moments. Magnetic moments aligned opposite the field are represented in light grey, while those already reversed appear in dark grey. Black regions represent the domain walls. (a) Reversion starts at the central wire, where domain walls nucleate at the extremes and propagate towards the center. (b) In two of the border wires there is also the nucleation of domain walls in the central part. These walls propagate towards the tips, merging with the ones generated there.

ered, becoming more stable. The reversal process starts easily and simultaneously in two opposite external wires, separated by a distance equal to $2D$. This intermediate configuration is very favorable since comprises six antiferromagnetic bonds between nearest-neighboring wires, and four between next-nearest-neighboring wires. The reversal process continues with two other pairs of opposite external wires, being the central wire the last one to reverse, exhibiting a coercivity that is even larger than the one for a noninteracting system. For $D>150$ nm the array may be considered as a noninteracting one, with all the wires reversing essentially at the same time since they are identical and independent.

IV. CONCLUSIONS

In this paper we have used a scaling technique combined with Monte Carlo simulations in order to investigate the reversal of a hexagonal array of seven wires. The possibility of such a scale reduction increases considerably the applicability of numerical simulations to material science in general. This method allows us to consider the internal structure of each wire during the reversal process. With the proposed simulation scheme we were able to reproduce experimental results for Ni nanowires, that is the decrease in remanence and coercivity as interaction becomes stronger.[24] The shear observed in the hysteresis curve can be attributed to interaction among wires, a result supported by independent simulations and analytical calculations by other authors. The existence of a maximum in our coercivity curve (Fig. 2) resides in the definition of a particular reversal order of the wires determined mainly by the dipolar interaction. We believe that the maximum observed in experimental curves[25] is originated by a similar process. The positional disorder of the wires, which is always present in real macroscopic arrays, may create local cells generating blocking of innermost wires. Since our wires had no internal disorder, we can discard the influence of such effect in the behavior of coercivity. Our results show that strongly interacting systems experience a reversal process much slower than noninteracting.

ACKNOWLEDGMENTS

This work was partially supported by FONDECYT under Grant No. 1050013 and Grant No. 7050273, and from the Millennium Science Nucleus "Condensed Matter Physics" P02-054F, and CNPq, PIBIC/UFRJ, FAPERJ, PROSUL Program, and Instituto de Nanociências/MCT of Brazil. One of the authors, S.A., acknowledges the support from CONICYT, Dirección de Postgrado, Universidad de Santiago de Chile, and PROSUL, which financed his stay at Universidade Federal do Rio de Janeiro.

[1] J. N. Chapman, P. R. Aitchison, K. J. Kirk, S. McVitie, J. C. S. Kools, and M. F. Gillies, J. Appl. Phys. **83**, 5321 (1998).
[2] C. A. Ross, Henry I. Smith, T. Savas, M. Schattenburg, M. Farhoud, M. Hwang, M. Walsh, M. C. Abraham, and R. J. Ram, J. Vac. Sci. Technol. B **17**, 3168 (1999).
[3] L. C. Sampaio, E. H. C. P. Sinnecker, G. R. C. Cernicchiaro, M. Knobel, M. Vázquez, and J. Velázquez, Phys. Rev. B **61**, 8976 (2000).
[4] M. Knobel, L. C. Sampaio, E. H. C. P. Sinnecker, P. Vargas, and D. Altbir, J. Magn. Magn. Mater. **249**, 60 (2002).
[5] Riccardo Hertel, J. Appl. Phys. **90**, 5752 (2001).
[6] Riccardo Hertel and Jürgen Kirschner, Physica B **343**, 206 (2004).
[7] Liviu Clime, Petru Ciureanu, and Arthur Yelon, J. Magn. Magn. Mater. **297**, 60 (2006).
[8] K. Nielsch, R. B. Wehrspohn, J. Barthel, J. Kirschner, U. Gösele, S. F. Fischer, and H. Kronmüller, Appl. Phys. Lett. **79**, 1360 (2001).
[9] M. Vázquez, K. Pirota, J. Torrejo, M. Hernández-Vélez, and D. Navas, J. Magn. Magn. Mater. **294**, 395 (2005).
[10] D. J. Sellmyer, M. Zheng, and R. Skomski, J. Phys.: Condens. Matter **13**, R433 (2001).
[11] J. d'Albuquerque e Castro, D. Altbir, J. C. Retamal, and P. Vargas, Phys. Rev. Lett. **88**, 237202 (2002).
[12] P. Vargas, D. Altbir, and J. d'Albuquerque e Castro, Phys. Rev. B **73**, 092417 (2006).
[13] J. Mejia-Lopez, P. Soto, and D. Altbir, Phys. Rev. B **71**, 104422 (2005).
[14] C. Kittel, *Introduction to Solid State Physics* (John Wiley & Sons, New York, 2004).
[15] U. Nowak, R. W. Chantrell, and E. C. Kennedy, Phys. Rev. Lett. **84**, 163 (2000).
[16] C. S. M. Bastos, M. Bahiana, W. C. Nunes, M. A. Novak, D. Altbir, P. Vargas, and M. Knobel, Phys. Rev. B **66**, 214407 (2002).
[17] J. P. Pereira Nunes, M. Bahiana, and C. S. M. Bastos, Phys. Rev. E **69**, 056703 (2004).
[18] K. Binder and D. W. Heermann, *Monte Carlo Simulation in Statistical Physics* (Springer, New York, 2002).
[19] B. D. Cullity, *Introduction to Magnetic Materials* (Addison-Wesley, Reading, MA, 1972).
[20] E. O. Samwel, P. R. Bissell, and J. C. Loddre, J. Magn. Magn. Mater. **115**, 327 (1992).
[21] Y. Ishii and M. Sato, J. Magn. Magn. Mater. **82**, 309 (1989).
[22] T. G. Sorop, C. Untiedt, F. Luis, M. Kroll, M. Rasa, and L. J. de Jongh, Phys. Rev. B **67**, 014402 (2003).
[23] M. Hwang, M. Farhoud, Y. Hao, M. Walsh, C. A. Ross, T. A. Savas, and H. I. Smith, IEEE Trans. Magn. **36**, 3173 (2000).
[24] M. Vázquez, M. Hernández-Vélez, K. Pirota, A. Asenjo1, D. Navas, J. Velázquez, P. Vargas, and C. Ramos, Eur. Phys. J. B **40**, 489 (2004).
[25] M. Zheng, L. Menon, H. Zeng, Y. Liu, S. Bandyopadhyay, R. D. Kirby, and D. J. Sellmyer, Phys. Rev. B **62**, 12282 (2000).